

## Developing a smart structure using integrated DDA/ISMP and semi-active variable stiffness device

Kaveh Karami<sup>\*1</sup>, Satish Nagarajaiah<sup>2</sup> and Fereidoun Amini<sup>3</sup>

<sup>1</sup>Faculty of Department of Civil Engineering, University of Kurdistan, Sanandaj, Iran

<sup>2</sup>Faculty of Departments of Civil and Environmental Engineering, and Mechanical Engineering and Material Science, Rice University, Houston, USA

<sup>3</sup>Faculty of School of Civil Engineering, Iran University of Science & Technology, Tehran, Iran

(Received December 29, 2015, Revised August 20, 2016, Accepted August 23, 2016)

**Abstract.** Recent studies integrating vibration control and structural health monitoring (SHM) use control devices and control algorithms to enable system identification and damage detection. In this study real-time SHM is used to enhance structural vibration control and reduce damage. A newly proposed control algorithm, including integrated real-time SHM and semi-active control strategy, is presented to mitigate both damage and seismic response of the main structure under strong seismic ground motion. The semi-active independently variable stiffness (SAIVS) device is used as semi-active control device in this investigation. The proper stiffness of SAIVS device is obtained using a new developed semi-active control algorithm based on real-time damage tracking of structure by damage detection algorithm based on identified system Markov parameters (DDA/ISMP) method. A three bay five story steel braced frame structure, which is equipped with one SAIVS device at each story, is employed to illustrate the efficiency of the proposed algorithm. The obtained results show that the proposed control algorithm could significantly decrease damage in most parts of the structure. Also, the dynamic response of the structure is effectively reduced by using the proposed control algorithm during four strong earthquakes. In comparison to passive on and off cases, the results demonstrate that the performance of the proposed control algorithm in decreasing both damage and dynamic responses of structure is significantly enhanced than the passive cases. Furthermore, from the energy consumption point of view the maximum and the cumulative control force in the proposed control algorithm is less than the passive-on case, considerably.

**Keywords:** structural health monitoring; real-time damage detection algorithm based on identified system Markov parameters; variable stiffness device; semi-active control; system identification; damage control

### 1. Introduction

In the past two decades most research has been conducted in the field of SHM and vibration control of structure, separately. In recent years many researchers have studied integrated SHM and vibration control. Hitherto, all research on the integration of vibration control and health monitoring of structures conducted use control devices and control algorithms to enable system identification and damage detection. Integrating modal frequency sensitivity analysis and feedback

---

\*Corresponding author, Assistant Professor, E-mail: [ka.karami@uok.ac.ir](mailto:ka.karami@uok.ac.ir)

control lead to provide detecting damage (Ray and Tian 1999, Ray, Koh *et al.* 2000). Gattulli and Romeo (2000) used a direct adaptive control algorithm for both vibration response reduction and damage detection in structural systems. Kim (2002) presented an integrated technique which provides substantial vibration reductions, while detecting damage on the active beam structure, simultaneously. Viscardi and Lecce (2002) used piezoelectric devices for both active vibro-acoustic control and damage detection in a typical aeronautical structure. Sun and Tong (2003) proposed a closed loop control based damage detection scheme for small damage detection in smart beam. Xu and Chen (2008) presented a damage detection procedure in the time domain using additional stiffness provided by semi-active friction damper. Huang *et al.* (2012) introduced a similar damage detection procedure as the proposed method by Xu and Chen (2008), but in the frequency domain. Chu and Lo (2009) proposed a real-time model reference adaptive identification technique based on the online parameter estimation of model reference adaptive structural control algorithm. Chen, Xu *et al.* (2010) presented a general approach in the time domain for integrating vibration control and health monitoring of a structure to accommodate various types of control devices and online damage detection. Bitaraf, Barroso *et al.* (2010) proposed a method to mitigate damage impact on structural response and force the damaged structure to behave like an undamaged structure using adaptive control. Karami and Amini (2012) introduced an algorithm, including integrated online SHM and a 20t MR damper as a semi-active control device, to reduce both damage and seismic response of the main structure due to seismic disturbance. Amini, Mohajeri *et al.* (2015) proposed an integrated SHM and semi-active control scheme to reduce dynamic response of damaged isolated structures. Also, a new scheme has been presented by Karami and Akbarabadi (2016) to develop a smart structure by integrating subspace-based damage detection method and semi-active control strategy.

Designing the structure to be much too stiff using control devices in order to prevent the occurrence of damage under strong earthquakes is not a good idea from an economic point of view (Amini and Karami 2011, O'Byrne, Ghosh *et al.* 2014, Sun, Feng *et al.* 2015, Cha and Buyukozturk 2015). Also, if control devices with constant stiffness are applied to reduce displacement during strong earthquakes, the frequency and the acceleration response of the structure maybe increased. Increasing of the internal force due to high acceleration response can cause increased damage in elements of the structure. On the other hand inappropriate stiffness variation based on measured dynamic response may affect the performance of the system adversely, due to incorrect determination of the necessary stiffness of the control device. So, appropriate variation of the stiffness of the control device based on detected damage in structure is one of the most important issues addressed in this study.

In this paper, application of the integrated online SHM and semi-active control strategy is presented to reduce both damage and dynamic response of the main structure under strong seismic ground motion. In other words, in this study the online SHM is used to enhance structural vibration control unlike the prior research studies. Nonlinear dynamic response of the main structure is measured by data acquisition system during strong excitation. The stiffness loss in structure is determined using damage detection algorithm based on identified system Markov parameters (DDA/ISMP) method - the damage detection method proposed by Amini and Karami (2012) - based on measured data. Also, the semi-active variable stiffness device (SAIVS) is used to compensate for damage/loss of stiffness and reduce dynamic response of the structure. A new semi-active control algorithm is developed based on real-time damage tracking of structure by DDA/ISMP method. The feasibility of the proposed algorithm is demonstrated through a detailed numerical investigation on a five story steel braced frame structure with a SAIVS device at each

story level. Four strong earthquakes are considered. It is shown that the proposed controller is effective in reducing both damage and seismic response of the structure.

## 2. Damage detection

In this investigation, the real-time damage in structural elements and reduction of lateral story stiffness of the main structure is identified using the DDA/ISMP method, proposed by Amini and Karami (2012), which is reviewed here, briefly. The DDA/ISMP is a new approach for global/local damage detection (identifying the location, type and quantity of damage) in finite element model of the building structure using limited sensors. In this method, the identification equations of structural parameters (such as mass, damping and stiffness matrices) are directly related to the Markov parameters, locations of actuators and sensors. Also, there is no explicit relation between DDA/ISMP and mode shapes. Therefore in comparison to the other usual methods, DDA/ISMP has two important advantages: (a) It is not necessary to install a sensor at each DOF to identify mode shapes. Thus, the stiffness of entire structure elements can be extracted using the limited number of sensors and actuators; (b) The local identification of the system is possible by recognizing the suitable locations of the sensors and actuators corresponding to the specified elements of the structure.

Usually, some parts of the structure experience damage during large environmental excitation. Here, damage means reduction (loss) in the lateral story stiffness. While, the finite element model of structure is used in this study, thus it is necessary to determine stiffness of all structural elements. Because, the lateral story stiffness is calculated using all elements stiffness. In conclusion, the main reason of using the DDA/ISMP is achieving this goal.

In this technique, damage is detected based on the identified Markov parameters. The Markov parameters of system are identified from measured input and output data directly, using ERA/OKID (Juang, Phan *et al.* 1993, Juang 1994). The input and output data are measured by installing sensors at appropriate DOF. The equation of identified stiffness matrix corresponding to the structure with  $n$  number of DOF,  $r$  inputs and  $m$  outputs is obtained as follows

$$U_k = Y_B K_0 Y_I \tag{1}$$

Where

$$U_k = \tilde{Y}_3 (\tilde{Y}_2)^\dagger \tilde{Y}_3 - \tilde{Y}_4 \tag{2}$$

$$Y_B = \tilde{Y}_2 (B_u)^\dagger \tag{3}$$

$$Y_I = (C_m)^\dagger \tilde{Y}_2 \tag{4}$$

in which  $K_0$  with dimensions  $n$  by  $n$  is the stiffness matrix. The parameter  $\tilde{Y}_i$  with  $m \times r$  dimensions is the  $i^{\text{th}}$  identified system Markov parameter. The matrix  $B_u$  with dimensions  $n \times r$  indicates location of actuators. In this study the accelerations are considered as outputs; so, the installed sensors at the DOFs measure accelerations. The matrix  $C_m$  with dimension  $m$  by  $n$ , which are corresponding to accelerations, indicates the sensors location. The sign  $()^\dagger$  is the

pseudo inverse of matrix. The Eq. (1) is rewritten so that  $\mathbf{K}_0$  appears as an unknown column vector  $\mathbf{k}_0$  with dimension  $n^2 \times 1$  as follows

$$\mathbf{A}_k \mathbf{k}_0 = \mathbf{h}_k \tag{5}$$

$$\mathbf{A}_k = \mathbf{Y}_B \otimes \mathbf{Y}_I^T \tag{6}$$

$$\mathbf{k}_0 = \{k_{11} \ \dots \ k_{1n} \ | \ k_{21} \ \dots \ k_{2n} \ | \ \dots \ | \ k_{n1} \ \dots \ k_{nn}\}^T \tag{7}$$

$$\mathbf{h}_k = \{h_{11} \ \dots \ h_{1n} \ | \ h_{21} \ \dots \ h_{2n} \ | \ \dots \ | \ h_{n1} \ \dots \ h_{nn}\}^T \tag{8}$$

in which the matrix  $\mathbf{A}_k$  is the coefficient matrix with dimension  $mr$  by  $n^2$ . The sign  $\otimes$  is the Kronecker product. The element  $k_{ij}$  in the vector  $\mathbf{k}_0$  is corresponding to  $(i, j)^{th}$  element of matrix  $\mathbf{K}_0$ . The element  $h_{ij}$  in the  $\mathbf{h}_k$  vector ( $mr \times 1$ ) is corresponding to  $(i, j)^{th}$  element of  $\mathbf{U}_k$  matrix. The elements of stiffness matrix are determined by using Eq. (5). But, to preserve the sparsity property of the identified stiffness matrix, the sparsity is considered as a constraint condition. By eliminating all of the known zero elements from  $\mathbf{k}_0$  and deleting entire corresponding columns in matrix  $\mathbf{A}_k$  the sparsity property can be achieved. If there are  $\gamma$  zero elements in matrix  $\mathbf{K}_0$ , the Eq. (5) is simplified as follows

$$\mathbf{A}_k^m \mathbf{k}_0^m = \mathbf{h}_k \tag{9}$$

The vector  $\mathbf{k}_0^m$  with  $(n^2 - \gamma) \times 1$  dimension is constructed by eliminating the zero elements of  $\mathbf{k}_0$  vector. The matrix  $\mathbf{A}_k^m$  with  $mr \times (n^2 - \gamma)$  dimension is obtained by deleting all the columns that multiply by  $k_{ij} = 0$ . Here, only the axial and bending stiffness of the buildings structural members are considered. So, the vector  $\mathbf{k}_0^m$  can be obtained as follows

$$\mathbf{k}_0^m = \mathbf{T}_f \mathbf{k}_0^z \tag{10}$$

$$\mathbf{k}_0^z = \{k_{A_1} \ k_{B_1} \ | \ k_{A_2} \ k_{B_2} \ | \ \dots \ | \ k_{A_\Omega} \ k_{B_\Omega}\}^T \tag{11}$$

in which  $k_{A_i}$  and  $k_{B_i}$  are the axial and bending stiffness corresponding to  $i^{th}$  frame element of the building structure which are defined as

$$k_A = EA_s L^{-1} \qquad k_B = EIL^{-1} \tag{12}$$

The parameters  $E$ ,  $I$ ,  $A_s$  and  $L$  are modulus of elasticity, moment of inertia, cross section and element length, respectively. Also,  $\Omega$  is the numbers of frame elements of structure. The dimension of vector  $\mathbf{k}_0^z$  is  $2\Omega \times 1$ . The matrix  $\mathbf{T}_f$  is the transformation matrix with dimension  $(n^2 - \gamma)$  by  $2\Omega$  which was proposed by Amini and Karami (2012). By substituting the Eq. (10) into the Eq. (9) yields

$$\mathbf{A}_k^m \mathbf{T}_f \mathbf{k}_0^z = \mathbf{h}_k \quad (13)$$

The minimum norm least squares solution for  $\mathbf{k}_0^z$  is

$$\mathbf{k}_0^z = \left( \mathbf{A}_k^m \mathbf{T}_f \right)^\dagger \mathbf{h}_k \quad (14)$$

The axial and bending stiffness of entire frame elements of structure are identified using Eq. (14). The damage size ( $\Delta \mathbf{k}^z$ ), is defined as the absolute value of the difference between the identified initial stiffness (undamaged stiffness),  $\mathbf{k}_0^z$ , and the identified damaged stiffness,  $\mathbf{k}_d^z$ , divided by identified initial stiffness as follows

$$\Delta \mathbf{k}^z (\%) = \frac{|\mathbf{k}_0^z - \mathbf{k}_d^z|}{\mathbf{k}_0^z} \times 100 \quad (15)$$

Assembling a physical model of the main structure is achievable when the stiffness properties of all structural elements are identified. The total lateral stiffness of each story is calculated using the physical model of the main structure. The damage in the story or lateral stiffness reduction at any time step is obtained using the following equation

$$kp_{(t)} (\%) = \frac{|ksd_{(t)}|}{k_{(0)}} \times 100 \quad (16)$$

where

$$ksd_{(t)} = k_{(0)} - k_{(t)} \quad (17)$$

in which  $k_{(0)}$  is the initial (undamaged) story lateral stiffness,  $k_{(t)}$ ,  $ksd_{(t)}$  and  $kp_{(t)}$  are story lateral stiffness, story lateral stiffness loss and damage in story lateral stiffness at time  $t$ , respectively. Finally, the damage location, type and quantity in element and story lateral stiffness of the main structure are detected.

### 3. Semi-active variable stiffness device (SAIVS)

A question may be raised in mind that how the lateral story stiffness loss could be compensated. In this case, a semi-active control device with capability of changing its stiffness continuously is the solution. Hence, the semi-active variable stiffness device (SAIVS) is suitable option in order to compensate for damage/loss of stiffness. For the first time Nagarajaiah (2000) has developed a new and innovative SAIVS device with capability of changing its stiffness continuously, independently and smoothly between minimum and maximum stiffness. The application of SAIVS in a great deal of structural controlled systems was evaluated (Varadarajan and Nagarajaiah 2004, Nagarajaiah and Varadarajan 2005, Narasimhan and Nagarajaiah 2005, Nagarajaiah and Sahasrabudhe 2006, Nagarajaiah and Sonmez 2007). Fig. 1 depicts the mechanical model for the

SAIVS device which consists of four spring elements arranged in a plane rhombus configuration with pivot joints at the vertices.

The joint 1 can move only in vertical direction. The joint 2 can move in both horizontal and vertical direction. Also, the joints 3 and 4 can move only in horizontal direction. The aspect ratio of the rhombus configuration of the SAIVS device is reconfigured using a linear electromechanical actuator. The aspect ratio changes between passive on (the springs are nearly horizontal in closed configuration) and passive off (the springs are nearly vertical in open configuration) situations, producing maximum and minimum stiffness, respectively. The variable stiffness of the SAIVS device is obtained by the following equation

$$ks_{(t)} = ke \cdot \cos^2(\theta_{(t)}) \quad (18)$$

where  $ks_{(t)}$  is the time varying stiffness of the device, and  $ke = 28000$  kN/m is the constant spring stiffness of each spring element,  $\theta_{(t)}$  is the time varying angle of the spring elements with the horizontal in any position of the device as shown in Fig. 1. The angle of the spring is a function of the controller output command voltage to the linear actuator of the device. For a specific position the force developed at any time,  $Fs_{(t)}$ , in the device is given by

$$Fs_{(t)} = ks_{(t)}\Delta s_{(t)} \quad (19)$$

where  $\Delta s_{(t)}$  is the relative displacement between joints 1 and 2 in the x direction. The device generates a certain  $Fs$  for a particular angle. For example, when  $\theta = 20.27^\circ$ ,  $ks_{\max} = 24640$  kN/m and when  $\theta = 76.60^\circ$ ,  $ks_{\min} = 1502$  kN/m. For intermediate  $\theta$ , the stiffness varies between  $ks_{\max}$  and  $ks_{\min}$ , continuously. The device is linear but the SAIVS behavior is hysteretic. The angle is varied, so that the stiffness continuously varies, resulting in hysteretic behavior, leading to additional energy dissipation. In this study, the necessary device stiffness is related to lateral story stiffness loss based on real-time story damage tracking of structure by DDA/ISMP method. So the input voltage to the linear electromechanical actuator is regulated to achieve desirable device configuration with appropriate stiffness.

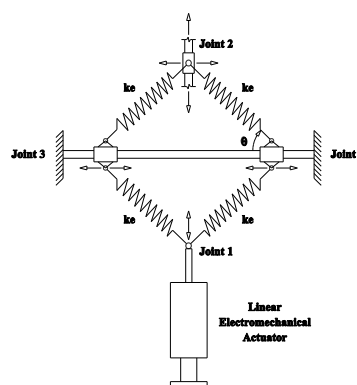


Fig. 1 The mechanical model of the SAIVS device

#### 4. SAIVS control algorithm based on identified story damage

The appropriate stiffness produced by SAIVS device is obtained based on identified lateral story stiffness loss. The lateral story stiffness loss of the main structure varies during strong earthquake, at times suddenly. So, if the SAIVS device stiffness is equated to the lateral story stiffness loss based on real-time story damage tracking of the structure, resulting in nonsmooth changes in the SAIVS device stiffness, adverse effects in acceleration response of the main structure result. Narasimhan and Nagarajaiah (2005) considered a smoothing function,  $f_{(t)} = 2/(1 + e^{\alpha t})$ , to vary the SAIVS device stiffness from  $ks_{max}$  to  $ks_{min}$ . Hence, adequate time,  $\delta$ , needed for changing SAIVS device stiffness smoothly from  $ks_{max}$  to  $ks_{min}$  is achieved by the following equation

$$\delta = \alpha^{-1} \cdot \ln[(2ks_{max}/ks_{min}) - 1] \tag{20}$$

in which  $\alpha$  is a constant (a value of 4 is chosen for the current study). Usually, changing the SAIVS device stiffness from  $ks_{max}$  to  $ks_{min}$  takes a little time,  $\delta$ , which is approximately less than one Second. In Eq. (20), the parameter  $\alpha$  regulates the time  $\delta$ . In this study, considering  $\alpha = 4$  leads to  $\delta = 0.86$  Sec which is smaller than 1 Sec. If the SAIVS device is in the descending branch (changing from high stiffness to low stiffness) the proper SAIVS device stiffness at time  $t$ ,  $\tilde{ks}_{(t)}$ , is obtained by following equation

$$\tilde{ks}_{(t)} = 2ks_{max} [1 + e^{\alpha(\tau + \Delta t)}]^{-1} \tag{21}$$

where

$$\tau = \frac{1}{\alpha} \ln[(2ks_{max}/ks_{(t-1)}) - 1] \tag{22}$$

$ks_{(t-1)}$  is the SAIVS device stiffness at time  $t - \Delta t$ ,  $\Delta t$  is the time step and  $\tau$  is time situation of the SAIVS device at  $ks_{(t-1)}$ . If the SAIVS device is in the ascending branch (changing from low stiffness to high stiffness) the proper SAIVS device stiffness at time  $t$ ,  $\tilde{ks}_{(t)}$ , is obtained by following equation

$$\tilde{ks}_{(t)} = \delta_1 [\delta_2 + e^{-\alpha(\tau + \Delta t)}]^{-1} \tag{23}$$

where

$$\delta_1 = (1 - e^{-\alpha\delta}) [ks_{min}^{-1} - ks_{max}^{-1}]^{-1} \tag{24}$$

$$\delta_2 = \delta_1 ks_{min}^{-1} - 1 \tag{25}$$

$$\tau = -\alpha^{-1} \cdot \ln(\delta_1 k_{S(t-1)}^{-1} - \delta_2) \quad (26)$$

Eight constraints should be considered to prevent sudden changes in the SAIVS device stiffness. The sudden change in the SAIVS device stiffness has negative effects on the proposed control performance; extra acceleration is exerted in the story due to sudden changing in the SAIVS stiffness. Therefore, the internal forces in the structural members are increased which is not desirable. The considered constraints, including:

1. If (a) the necessary SAIVS device stiffness at time  $t$  is larger than the SAIVS device stiffness at time  $t - \Delta t$ ; and (b) the SAIVS device stiffness at time  $t - \Delta t$  is larger than the SAIVS device stiffness at time  $t - 2\Delta t$  (Fig. 2.1); then, the necessary SAIVS device stiffness at time  $t$  is proper and the SAIVS device stiffness at time  $t - \Delta t$  can be increased to reach to the proper value at time  $t$  (Fig. 2.1).
2. If (a) the necessary SAIVS device stiffness at time  $t$  is larger than the SAIVS device stiffness at time  $t - \Delta t$ ; and (b) the SAIVS device stiffness at time  $t - \Delta t$  is smaller than the SAIVS device stiffness at time  $t - 2\Delta t$  (Fig. 2.2); then, the proper SAIVS device stiffness at time  $t$  is equated to the SAIVS device stiffness at time  $t - \Delta t$  (Fig. 2.2).
3. If (a) the necessary SAIVS device stiffness at time  $t$  is smaller than the SAIVS device stiffness at time  $t - \Delta t$ ; and (b) the SAIVS device stiffness at time  $t - \Delta t$  is smaller than the SAIVS device stiffness at time  $t - 2\Delta t$  (Fig. 2.3); then, the necessary SAIVS device stiffness at time  $t$  is proper and the SAIVS device stiffness at time  $t - \Delta t$  can be decreased to reach to the proper value at time  $t$  (Fig. 2.3).
4. If (a) the necessary SAIVS device stiffness at time  $t$  is smaller than the SAIVS device stiffness at time  $t - \Delta t$ ; (b) the SAIVS device stiffness at time  $t - \Delta t$  is larger than the SAIVS device stiffness at time  $t - 2\Delta t$  (Fig. 2.4); and (c) the necessary SAIVS device stiffness at time  $t$  is proper if the following condition is satisfied

$$\frac{1}{\beta} \sum_{j=1}^{\beta} k_{p(t-j)} \leq \varepsilon_1 \quad (27)$$

where

$$\beta = \delta / (2 \cdot \Delta t) \quad (28)$$

in which  $k_{p(t-j)}$  is the damage in story lateral stiffness at time  $t - j\Delta t$  and  $\varepsilon_1$  is a constant; then, the SAIVS device stiffness at time  $t - \Delta t$  can be decreased to reach to the proper value at time  $t$  (Fig. 2.4). The Eq. (27) determines the average damage in story lateral stiffness at  $\beta$  pervious time steps. It is compared with a constant at each time step to evaluate the recent (not instantaneous) situation of the structure. In other words, the Eq. (27) plays the role of a temporary memory which saves the recent situation of structure from damage occurrence point of view, during excitation. Due to this, the possibility of checking the robustness of the controller is obtained via this comparison. Therefore, the parameter  $\varepsilon_1$  should be set to a small value to avoid the decrease in the SAIVS device stiffness. If  $\varepsilon_1$  set to a high value, the SAIVS device stiffness can be decreased easily

which lead to make the control system as Passive off case; also, equating  $\varepsilon_1$  to zero makes the SAIVS device to behave in Passive on case which both are not desirable. Selecting a value between 1 to 3 percent can be a rational choice for the parameter  $\varepsilon_1$ . Thus, a value of 2% is chosen for the current study.

5. If (a) the necessary SAIVS device stiffness at time  $t$  is smaller than the SAIVS device stiffness at time  $t - \Delta t$ ; (b) the SAIVS device stiffness at time  $t - \Delta t$  is larger than the SAIVS device stiffness at time  $t - 2\Delta t$  (Fig. 2.5); and (c) if the following condition is satisfied

$$\varepsilon_1 < \frac{1}{\beta} \sum_{j=1}^{\beta} k p_{(t-j)} \leq \varepsilon_2 \tag{29}$$

then, the proper SAIVS device stiffness at time  $t$  is equated to the SAIVS device stiffness at time  $t - \Delta t$  (Fig. 2.5).  $\varepsilon_2$  is a constant (a value of 15% is chosen for the current study).

6. If (a) the necessary SAIVS device stiffness at time  $t$  is smaller than the SAIVS device stiffness at time  $t - \Delta t$ ; (b) the SAIVS device stiffness at time  $t - \Delta t$  is larger than the SAIVS device stiffness at time  $t - 2\Delta t$  (Fig. 2.6); and (c) if the following condition is satisfied

$$\varepsilon_2 < \frac{1}{\beta} \sum_{j=1}^{\beta} k p_{(t-j)} \tag{30}$$

then, the necessary SAIVS device stiffness at time  $t$  is not proper and the SAIVS device stiffness at time  $t - \Delta t$  should be increased to reach to the proper value at time  $t$  (Fig. 2.6).

7. If (a) the necessary SAIVS device stiffness at time  $t$  is  $k_{s_{min}}$ ; (b) the SAIVS device stiffness at time  $t - \Delta t$  is  $k_{s_{min}}$  too (Fig. 2.7); and (c) if the condition in Eq. (27) is satisfied then, the necessary SAIVS device stiffness at time  $t$  is proper (Fig. 2.7) and retained the same.

8. If (a) the necessary SAIVS device stiffness at time  $t$  is  $k_{s_{min}}$ ; (b) the SAIVS device stiffness at time  $t - \Delta t$  is  $k_{s_{min}}$  too (Fig. 2.8); and (c) if the condition in Eq. (27) is not satisfied or the damage in story lateral stiffness at time  $t$  is larger than a constant  $\varepsilon_3$  (a value of 5% is chosen for the current study); then, the necessary SAIVS device stiffness at time  $t$  is not proper and the SAIVS device stiffness at time  $t - \Delta t$  should be increased to reach to the proper value at time  $t$  (Fig. 2.8).

The block diagram of the proposed SAIVS controller algorithm based on identified damage is shown in Fig. 3.

### 5. Proposed algorithm including online DDA/ISMP and SAIVS device control

In this investigation, proper variation of the SAIVS device stiffness based on identified story damage is the main issue. Here, a new algorithm including integrated online DDA/ISMP method

and SAIVS device control is proposed to reduce both damage and dynamic response of the main structure during strong ground motion. Usually, the main structure responds in the nonlinear zone of its behavior during strong earthquake. In this study, a non-experimental investigation, the nonlinear behavior of the main structure is obtained by simulation. For this purpose, nonlinear analysis is performed at the simulation stage. One of the numerical methods which has been widely used in the literature is the Newmark's method (Chopra 1995, McGuire *et al.* 2000). In this study, the average acceleration method with modified Newton Raphson iteration is employed in the MDOF system. Also, the effects of both geometric and material nonlinearities are considered. The proposed algorithm including online DDA/ISMP method and SAIVS device control is shown in Fig. 4, which can be used to develop a smart structure system.

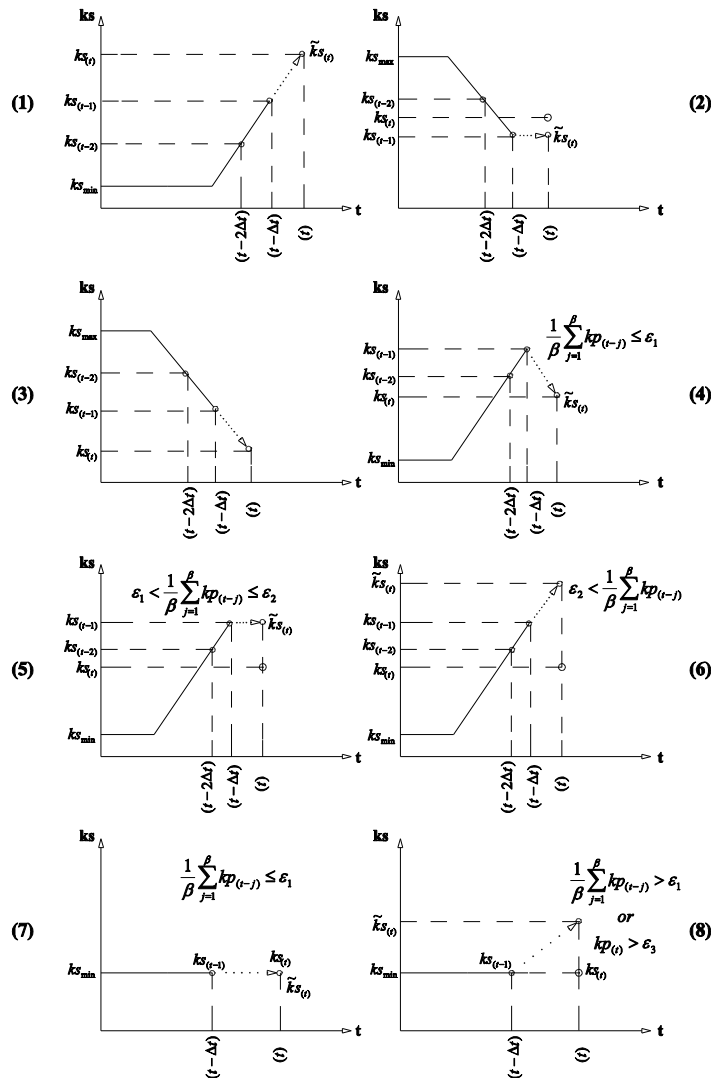


Fig. 2 Scheme changing of SAIVS device stiffness at specific cases

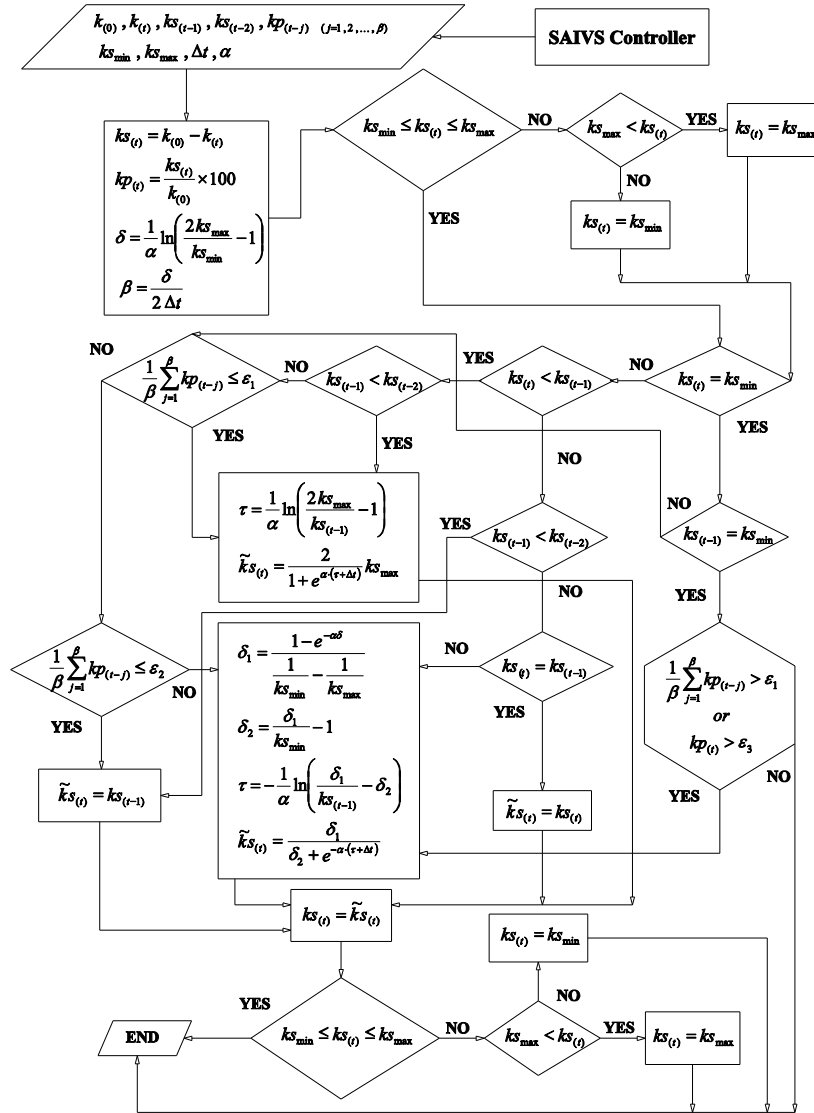
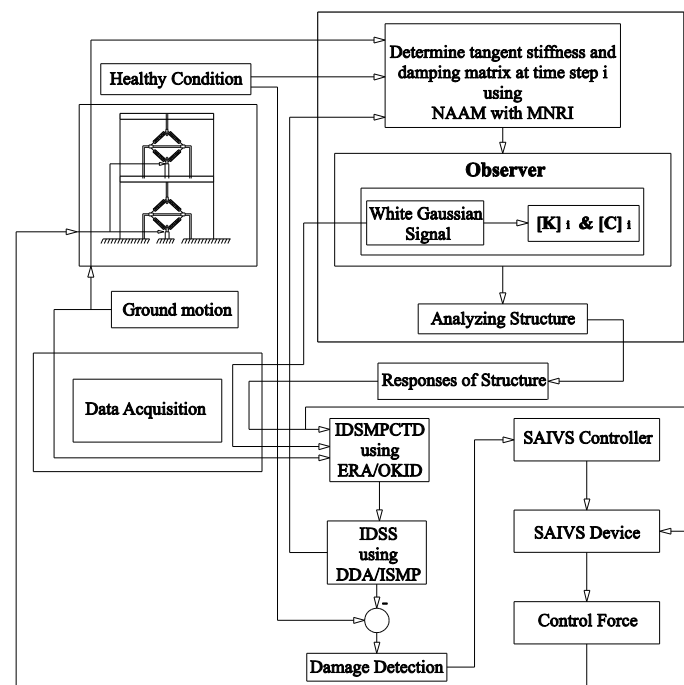


Fig. 3 The proposed SAIVS controller algorithm

The response of the main structure is measured by installing sensors at each appropriate DOF. The information about lateral story stiffness of the undamaged structure (healthy condition) is assumed to be available. This information is used as a data base for comparison with identified lateral story stiffness to detect damage during strong earthquake. The proposed algorithm contains a black box (simulated part), which corresponds to the nonlinear behavior simulation during strong ground motion. The tangent stiffness and damping matrix are calculated at each time step using the nonlinear analysis during the application of external force due to ground motion.

In this study, linear actuators are used to exert white Gaussian signal in the system

identification part. Therefore, the actuators are activated at beginning of the earthquake. The dynamic response of structure due to both earthquake and white Gaussian signals until the  $i^{th}$  time step is provided by analyzing the system. The necessary input/output data for the system identification part is supplied by the data acquisition/measurement system. The Markov parameters of the damaged structure in continuous-time domain are identified using ERA/OKID based on the input and output data until the  $i^{th}$  time step. Then, the damaged lateral story stiffness of the main structure is obtained using the identified Markov parameters of damaged system by the DDA/ISMP method. By comparing the original and damaged lateral story stiffness of the main structure the quantity and location of damage are calculated using Eq. (16).




---

#### Abbreviation

---

<b>IDSMPCTD</b>	Identified damaged system Markov parameters in continuous-time domain
<b>IDSS</b>	Identified damaged story lateral stiffness
<b>NAAM</b>	Newmark's average acceleration method
<b>MNRI</b>	Modified Newton Raphson iteration

---

Fig. 4 The proposed algorithm including integrated online SHM and semi-active control strategy

The proper SAIVS device stiffness is obtained based on lateral story stiffness loss in the SAIVS controller as shown in Fig. 3. The necessary control force is calculated based on the proper SAIVS device stiffness and measured relative displacement between joints 1 and 2, using Eq. (19). Afterwards, these steps are repeated for each time step.

In a regular vibration control strategy, the dynamic response of the structure is limited based on measured data. Also, there is no sense about behavior of the structure during excitation. We are facing to only measured response data and the information about probable occurred damage in the structure is not available. But, in the proposed method the SHM provides useful real time information about damage occurrence in the structure during excitation. In simple words, the remarkable difference and key point is that, identifying damage (location, type and quantity) in the proposed method plays the role of a memory which saves the recent situation of structure behavior from damage occurrence point of view during earthquake.

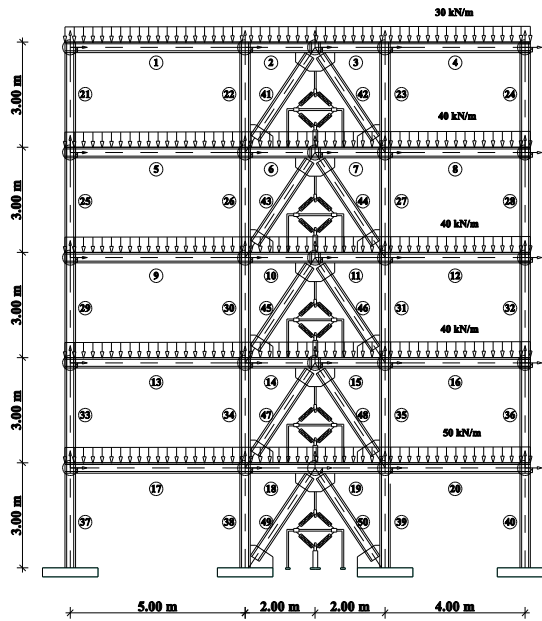


Fig. 5 The properties of 3 bay 5 story steel frame structure

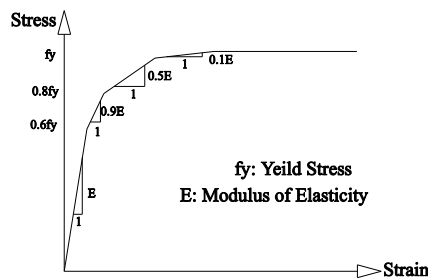


Fig. 6 The stress-strain curve of material used

Finally, if the damage appears during strong earthquake, the smart system detects location and quantity of damage by itself. Then it makes proper decision for regulating the SAIVS device stiffness to decrease both damage and system dynamic response. Therefore, creating a smart building by employing the proposed algorithm is achievable.

## 6. Numerical example

Here to illustrate the efficiency of the proposed algorithm a three bay five story steel braced frame structure, which includes 75 DOFs is employed. Fig. 5 depicts properties of finite element model of the five story structure. The distributed load on beams at story 1, 2, 3, 4 and 5 is 50, 40, 40, 40 and 30 (kN/m), respectively. As shown in Fig. 5, each node in the structure has two translational and one rotational DOF. In this study, 2 sensors are installed at each node to measure acceleration only in the horizontal and vertical directions. The section area ( $A_s$ ), the moment of inertia ( $I$ ) and the section modulus ( $W_s$ ) of elements used in the structure are given in the Table 1. Also, the mechanical parameters of structural element including modulus of elasticity, mass per unit volume and yield stress are  $1.999E+11$  (N/m<sup>2</sup>),  $7827$  (kg/m<sup>3</sup>) and  $2400$  (kg/cm<sup>2</sup>), respectively. The assumed stress-strain curve for elements material of the structure is shown in Fig. 6. In this example, a SAIVS device is installed at each story as a semi-active control device as shown in Fig. 5.

Table 1 The elements properties of the five story structure

Element NO.	Name	$A_s$ (m <sup>2</sup> )	$I$ (m <sup>4</sup> )	$W_s$ (m <sup>3</sup> )
14, 15	IPE180	2.3900E-03	1.3170E-05	1.4633E-04
10, 11, 18, 19	IPE200	2.8500E-03	1.9430E-05	1.9430E-04
4, 6, 7, 12	IPE240	3.9100E-03	3.8920E-05	3.2430E-04
1, 2, 3, 8, 16	IPE270	4.5900E-03	5.7900E-05	4.2889E-04
5, 9, 13, 20	IPE300	5.3800E-03	8.3560E-05	5.5707E-04
17	IPE330	6.2600E-03	1.1770E-04	7.1333E-04
23	HE100-B	2.6000E-03	4.5000E-06	9.0000E-05
22	HE120-B	3.4000E-03	8.6400E-06	1.4400E-04
27	HE140-B	4.3000E-03	1.5090E-05	2.1557E-04
24, 26, 28, 31, 32	HE160-B	5.4300E-03	2.4920E-05	3.1150E-04
21, 25, 30, 35, 36, 40	HE180-B	6.5300E-03	3.8310E-05	4.2567E-04
29	HE200-B	7.8100E-03	5.6960E-05	5.6960E-04
33, 34, 37, 39	HE220-B	9.1000E-03	8.0910E-05	7.3555E-04
38	HE240-B	1.0600E-02	1.1260E-04	9.3833E-04
41, 42	UNP160	2.4020E-03	9.2460E-06	1.1558E-04
43, 44	UNP200	3.2190E-03	1.9110E-05	1.9110E-04
45, 46, 47, 48	UNP220	3.7440E-03	2.6910E-05	2.4463E-04
49, 50	UNP240	4.2290E-03	3.5970E-05	2.9975E-04

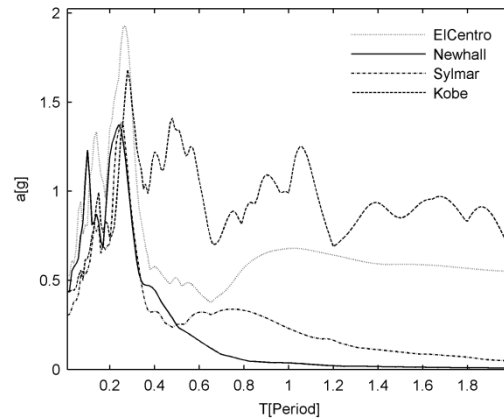


Fig. 7 The acceleration response spectrum of the applied earthquake records (damping ratio is 5%)

To evaluate the efficiency of the proposed algorithm and in order to consider the different intensity and duration in ground motion records, four strong earthquake records including (1) El-Centro-FN (Imperial Valley 10/15/79, Brawley Airport, USGS#5060, 225), (2) Newhall-FN (Northridge AFT 03/20/94, LA-Wonderland Ave, USC#17, 095), (3) Sylmar-FN (San Fernando 02/09/71, Fairmont DAM, CDMG#121, 056), and (4) Kobe-FP (Kobe 01/16/95, OSA, 090) with acceleration scaling factors 3.20, 8.90, 4.20 and 6.70, respectively are used. The acceleration response spectrum corresponding to the four earthquake records is shown in Fig. 7. Here, for comparison and verification, the structure equipped with three control strategy including passive off, in which the SAIVS device stiffness is equated to the constant value  $ks_{\min}$ , passive on, in which the SAIVS device stiffness is equated to the constant value  $ks_{\max}$ , and variable stiffness, in which the SAIVS device stiffness is varied based on the proposed control algorithm (with initial value  $ks_{\max}$ ), are assessed and compared with the uncontrolled structure.

The dynamic response time history at each story of controlled structure, including the proposed control algorithm, and uncontrolled structure under Sylmar earthquake is depicted in the Fig. 8. It is clear that, the proposed control strategy could effectively reduce the dynamic response of the structure within the whole earthquake duration. The maximum acceleration at story four only is slightly more than uncontrolled case but in the remaining duration of the earthquake the acceleration has been reduced. Fig. 9 shows the real-time monitoring of story drift and damage in lateral story stiffness of controlled and uncontrolled structure during Sylmar earthquake. The results reveal that the story drift and damage in lateral story stiffness are decreased using the proposed control algorithm.

The real-time monitoring of damage in the whole structure, at the cases with and without the proposed control algorithm, is shown through Figs. 10 to 12. The middle beams at initial stories have higher damage, because of large axial force due to braces, as shown in Fig. 10. The proposed control algorithm significantly decreases damage in beam elements, even in the middle beams at story 1 and 2 (El.14, 15, 18 and 19) which have permanent damage after 5 sec. Also, the damage in column and brace elements are reduced clearly in the controlled structure as demonstrated in Figs. 11 and 12, respectively.

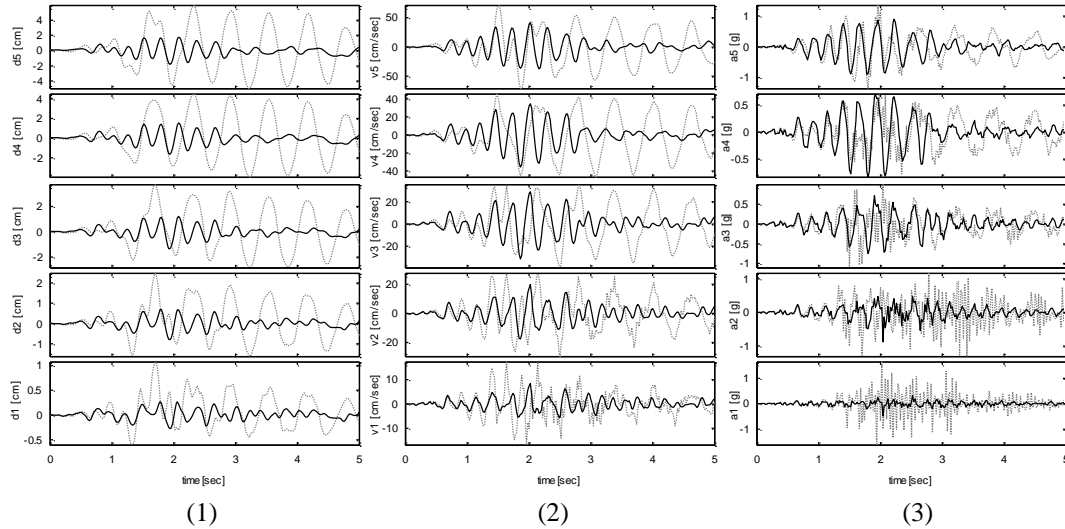


Fig. 8 The story dynamic response time history (1. displacement, 2. velocity and 3. acceleration) in two cases: Controlled (full line) and uncontrolled (dotted line) structure under Sylmar earthquake

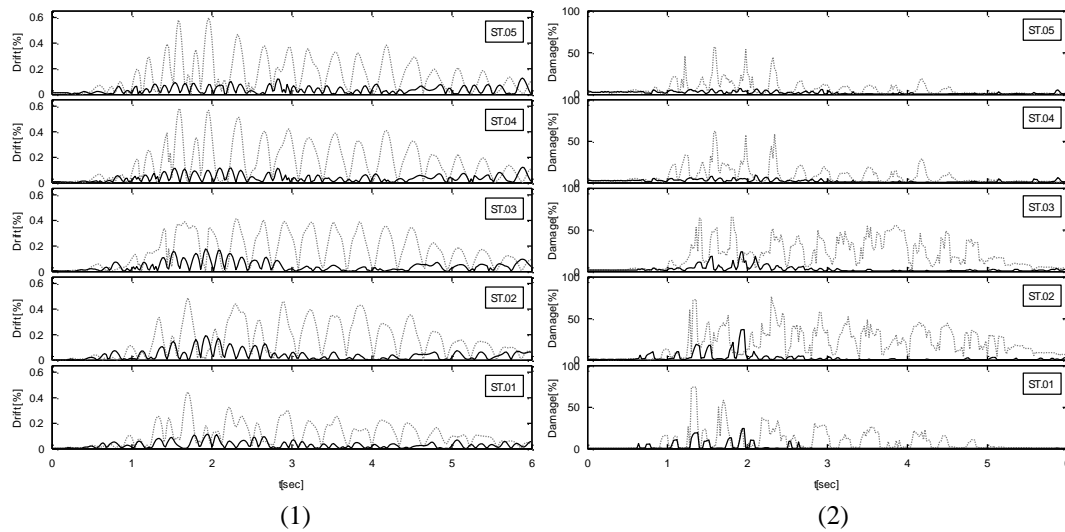


Fig. 9 Online monitoring of the story drift (1) and lateral stiffness damage (2) in two cases: Controlled (full line) and uncontrolled (dotted line) structure under Sylmar earthquake

Fig. 13 shows the activity of SAIVS device at each story due to the Sylmar earthquake. The time history of the SAIVS device stiffness is shown in Fig. 13.1. At the beginning of the earthquake, the SAIVS device stiffness at story 4 and 5 has the maximum stiffness, remaining constant until nearly 3 sec, after that the SAIVS device stiffness is reduced. But the SAIVS device stiffness at story 1, 2 and 3 has a different scenario; first, they are reduced to reach to the minimum

stiffness until 1 sec, and then they are increased. As shown in the Fig. 13.2, the control force time history of the SAIVS device, the maximum control force reaches  $\approx 83$  kN and occurs in the story 4 at time 2.24 sec. Also, the force-displacement response of the SAIVS device is presented in Fig. 13.3. It is clear that, the SAIVS device at each story has smooth and continuous behavior during the Sylmar earthquake.

Fig. 14 shows the real-time monitoring of story drift in two cases, controlled and uncontrolled structure, during Newhall, Kobe and El-Centro earthquake. The results reveal that the proposed control algorithm could effectively decrease the story drift due to three strong earthquakes.

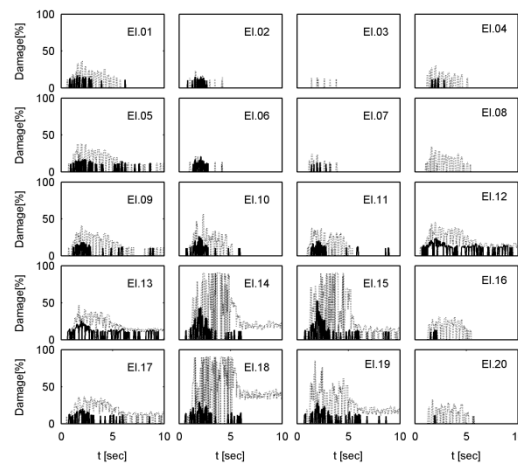


Fig. 10 Online monitoring of damage in the beam elements in two cases: Controlled (full line) and uncontrolled (dotted line) structure under Sylmar earthquake

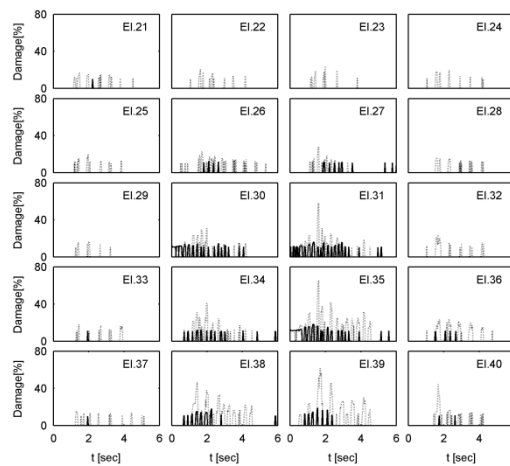


Fig. 11 Online monitoring of damage in the column elements in two cases: Controlled (full line) and uncontrolled (dotted line) structure under Sylmar earthquake

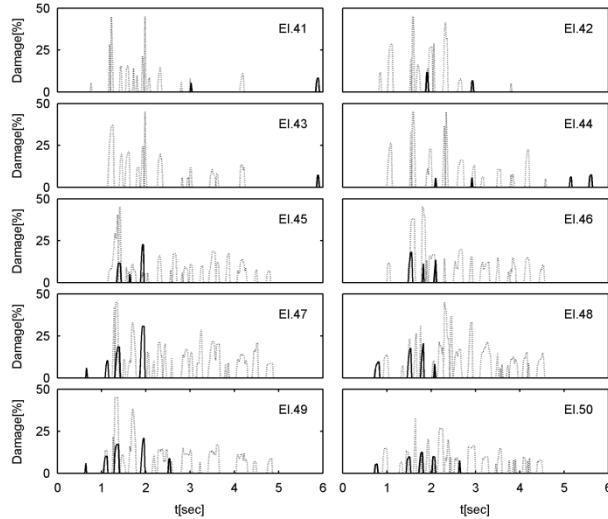


Fig. 12 Online monitoring of damage in the brace elements in two cases: Controlled (full line) and uncontrolled (dotted line) structure under Sylmar earthquake

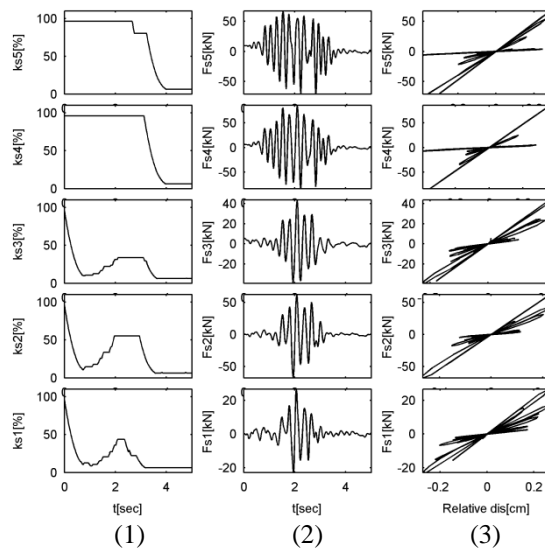


Fig. 13 Time histories of: 1. Stiffness (percentage of maximum value); 2. Control force in the SAIVS device; and 3. Force-displacement response of the SAIVS device at each story due to Sylmar earthquake

The time history of the SAIVS device stiffness at each story due to the Newhall, Kobe and El-Centro earthquake is depicted in Fig. 15. The SAIVS device stiffness at story 4 and 5 remained stable for a while and then dropped, at the beginning of the three earthquakes. But the SAIVS device stiffness at story 1, 2 and 3 are decreased to reach to the minimum stiffness, and then after

few seconds they start to be increase. The variation of stiffness in the SAIVS device during the Kobe earthquake is more, due to great deal of variation in damage.

Fig. 16 shows the dominant period time history of the example structure in the four cases: uncontrolled, passive off, variable stiffness (the proposed control algorithm) and passive on, in the four earthquakes. The period of the main structure is decreased by adding additional stiffness in the structure. Low period of the structure is not desirable in most of the strong earthquakes. In the passive on case the structure has the low period value, about 0.25 sec, during the four earthquakes as shown in Fig. 16.

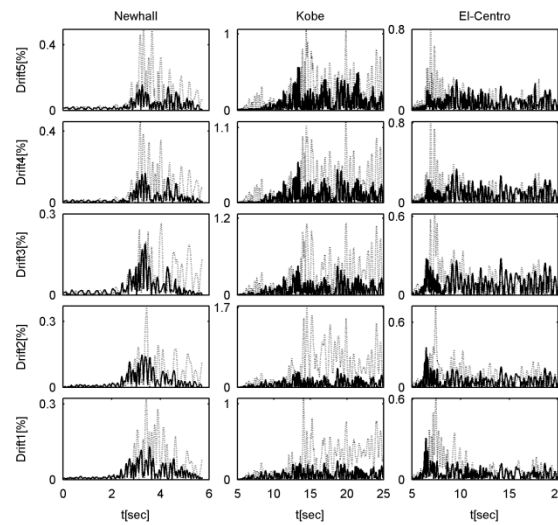


Fig. 14 Online monitoring of the story drift in two cases: Controlled (full line) and uncontrolled (dotted line) structure under Newhall, Kobe and El-Centro earthquake

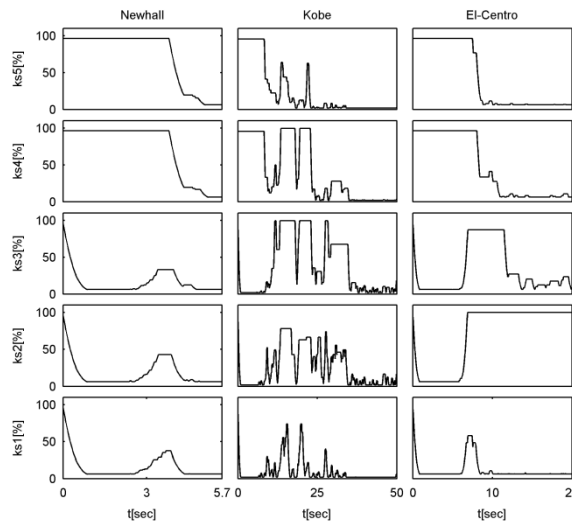


Fig. 15 Time history of stiffness in the SAIVS device (percentage of maximum value) at each story due to Newhall, Kobe and El-Centro earthquake

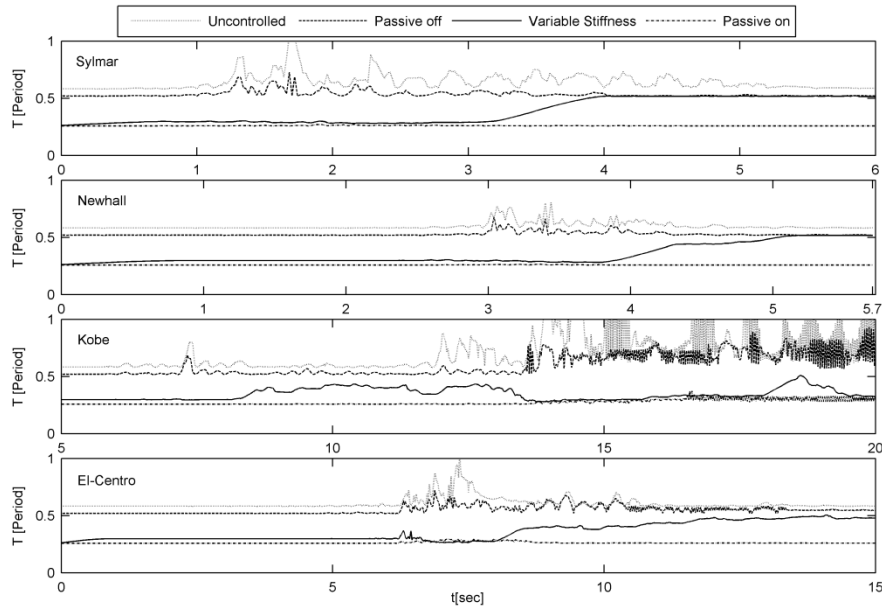


Fig. 16 Dominant period time history of the employed structure during four earthquakes

This value of period placed the structure in the acceleration sensitive zone of the spectrum (as demonstrated in Fig. 7), resulting in increasing acceleration leading to the exertion of large internal force in elements of the structure which tends to increase damage. On the other hand, since in the passive off case the minimum stiffness imparted by the SAIVS device is not sufficient to make structure stiff enough to prevent or reduce damage. Hence the period of the structure in this condition is always more in comparison to the case where the structure is equipped with passive on and variable stiffness control strategy. So, the best solution is varying the stiffness of the SAIVS device between passive on and passive off cases during large excitations.

In this investigation for making a comprehensive comparison, performance of the uncontrolled, passive off, variable stiffness and passive on cases is assessed in decreasing the 19 following items:

1. Cumulative value of absolute control force (C.CF.).
2. Maximum control force (M.CF.).
3. Period.
4. Cumulative column damage (C.Col.D.).
5. Cumulative brace damage (C.Br.D.)
6. Cumulative value of absolute story acceleration (C.St.Acc.).
7. Cumulative story damage (C.St.D.).
8. Cumulative beam damage (C.B.D.).
9. Cumulative value of absolute story velocity (C.St.Vel.).

10. Cumulative story drift (C.St.Dr.).
11. Cumulative value of absolute story displacement (C.St.Dis.).
12. Maximum story acceleration (M.St.Acc.).
13. Maximum story velocity (M.St.Vel.).
14. Maximum beam damage (M.B.D.).
15. Maximum column damage (M.Col.D.).
16. Maximum story displacement (M.St.Dis.).
17. Maximum story drift (M.St.Dr.).
18. Maximum story damage (M.St.D.).
19. Maximum brace damage (M.Br.D.).

The performance of  $i^{th}$  method,  $P_i^z(x_k)$ , in reduction of the item  $x_k$  at all stories during  $z^{th}$  earthquake is obtained using following equations

$$P_i^z(x_k) = \frac{1}{\text{Max}_{i=1}^4 \left( \sum_{j=1}^n P_{ij}^z(x_k) \right)} \left( \sum_{j=1}^5 P_{ij}^z(x_k) \right) \times 100 \tag{31}$$

where

$$P_{ij}^z(x_k) = 1 - (\bar{x}_k)_{ij}^z + \text{Min}_{i=1}^4 [(\bar{x}_k)_{ij}^z] \tag{32}$$

$$(\bar{x}_k)_{ij}^z = \frac{(x_k)_{ij}^z}{\text{Max}_{i=1}^4 [(x_k)_{ij}^z]} \quad ; \quad \begin{matrix} (i = 1, 2, \dots, 4) & \& & (j = 1, 2, \dots, 5) \\ (z = 1, 2, \dots, 4) & \& & (k = 1, 2, \dots, 19) \end{matrix} \tag{33}$$

in which, the variables  $(x_k)_{ij}^z$  and  $(\bar{x}_k)_{ij}^z$  are respectively value and normalized value of the item  $x_k$  at  $j^{th}$  story using  $i^{th}$  method during  $z^{th}$  earthquake. Also,  $P_{ij}^z(x_k)$  is the relative performance of  $i^{th}$  method in reduction of the item  $x_k$  at  $j^{th}$  story during  $z^{th}$  earthquake.

The performance of the four cases in the 19 items during Sylmar, Newhall, Kobe and El-Centro earthquake are shown in Fig. 17. The proposed control algorithm, variable stiffness case, has the highest performance in most of the considered items during the four earthquakes. The uncontrolled case only has the maximum performance in the C.CF., M.CF. and period items than the other cases, because there is no control force due to additional stiffness in the structure. So, the amount of necessary control force is zero and the structure behaves with the high period during the earthquakes. Unlike the uncontrolled case, the passive on case has the minimum performance in the C.CF., M.CF. and period items than the other cases, due to high amount of necessary control force. Also, the structure dominant period in the passive on case is less than the other cases.

During Sylmar earthquake, the proposed control algorithm has the maximum performance in reducing damage items including C.Col.D., C.St.D., C.B.D., M.B.D., M.Col.D., M.St.D. and

M.Br.D.; also, the variable stiffness case decreases dynamic response of the structure, with the best performance observed in the C.St.Acc., C.St.Vel., M.St.Acc., M.St.Vel., M.St.Dis. and M.St.Dr. items. The performance of the passive on case is more than the other cases only in decreasing the C.St.Dr. and C.St.Dis. items. The proposed control algorithm and passive on cases have the same performance in the C.Br.D item. In reducing the C.St.Acc. item, the performance of the passive off case is more than the uncontrolled and even the passive on case. The passive off case has the minimum performance in reduction of the M.Br.D. and M.St.Acc. items. In other words, the performance of uncontrolled case is more than the passive off case in decreasing these two items.

During Newhall earthquake, the proposed control algorithm has better performance than the passive and uncontrolled cases in the most of damage and dynamic response items. The proposed control algorithm has the best performance in the C.Col.D., C.Br.D., C.St.D., C.B.D., M.B.D., M.Col.D., M.St.D. and M.Br.D. items; also, the performance of the variable stiffness case in decreasing the C.St.Acc., M.St.Acc., M.St.Vel., M.St.Dis. and M.St.Dr. items is the maximum. The performance of the passive on case is more than the other cases only in reducing the C.St.Dis., C.St.Dr. and C.St.Vel. items. The performance of the passive off case is lower than the other cases, even than the uncontrolled case, in reduction of the M.St.Vel., C.St.Dis., C.St.Dr. and C.B.D. items.

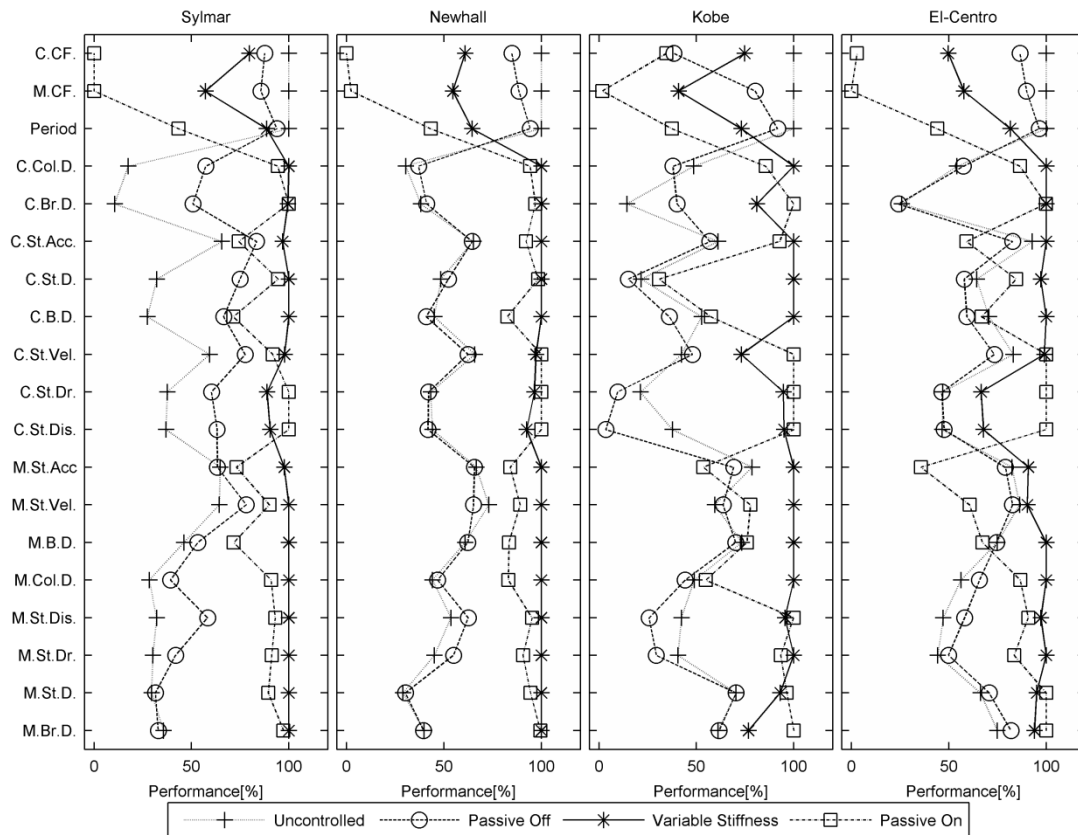


Fig. 17 Performance of the uncontrolled, passive off, variable stiffness and passive on cases in the 19 items during Sylmar, Newhall, Kobe and El-Centro earthquake

During Kobe earthquake, the proposed control algorithm has the maximum performance in reducing the items of damage including C.Col.D., C.St.D., C.B.D., M.B.D. and M.Col.D.; also, the variable stiffness case decreases dynamic response of the structure, with the best performance observed in the C.St.Acc., M.St.Acc., M.St.Vel. and M.St.Dr. items. The passive on case has the maximum performance in decreasing the M.Br.D., M.St.D., M.St.Dis., C.St.Dis., C.St.Dr., C.St.Vel. and C.Br.D. items; but the passive on case has the minimum performance, even lower than the uncontrolled case, in reducing the M.St.Acc. item. As shown in Fig. 17, the performance of passive off case is the minimum, even lower than the uncontrolled case, in decreasing most of the items.

During El-Centro earthquake, the proposed control algorithm has better performance than the passive and uncontrolled cases in the most of damage and dynamic response items. The proposed control algorithm has the best performance at the C.Col.D., C.Br.D., C.St.D., C.B.D., M.B.D. and M.Col.D. items; also, the performance of the variable stiffness case in decreasing the C.St.Acc., M.St.Acc., M.St.Vel., M.St.Dis. and M.St.Dr. items is the maximum. The performance of passive on case is more than the other cases in decreasing the M.Br.D., M.St.D., C.St.Dis., C.St.Dr. and C.St.Vel. items; but the performance of passive on case is the minimum, even lower than the uncontrolled case, in the M.B.D., M.St.Vel., M.St.Acc. and C.St.Acc. items. Also, in reducing the C.B.D. item the performance of passive on case is lower than the uncontrolled case. The performance of passive off case is the minimum in reduction of the C.St.Vel., C.B.D., C.St.D. and C.Br.D. items; also, the performance of passive off case is lower than even the uncontrolled case in decreasing the M.St.Vel., M.St.Acc. and C.St.Acc. items.

The total performance of four cases in the each 19 items is calculated by evaluating the obtained performance results from the Sylmar, Newhall, Kobe and El-Centro earthquake as follows

$$P_i(x_k) = \frac{1}{\text{Max}_{i=1}^4 \left( \sum_{z=1}^4 P_i^z(x_k) \right)} \left( \sum_{z=1}^4 P_i^z(x_k) \right) \times 100 \quad (34)$$

in which,  $P_i(x_k)$  is performance of  $i^{th}$  method in reduction of the item  $x_k$  at all stories during the four earthquakes. As shown in Fig. 18.1, the proposed control algorithm, variable stiffness case, has the maximum performance in reducing most of the considered items, clearly. The proposed control algorithm has the maximum performance in reducing the damage items including C.Col.D., C.St.D., C.B.D., M.B.D., M.Col.D. and M.St.D.; also, the variable stiffness case decreases dynamic response of the structure, with the best performance observed in the C.St.Acc., M.St.Acc., M.St.Vel., M.St.Dis. and M.St.Dr. items. The uncontrolled case only has the maximum performance in the C.CF., M.CF. and period items than the other cases. Unlike the uncontrolled case, the passive on case has the minimum performance in these three items and also, in decreasing the M.St.Acc. item. Although, the passive on case has the maximum performance in reducing the M.Br.D., C.St.Dis., C.St.Dr., C.St.Vel. and C.Br.D. items but in the other cases, the passive on case has the lower performance than the proposed control algorithm. The performance of passive off case is the minimum in reduction of the C.St.Dis. item and also in the M.St.Acc. item has the lower performance than the uncontrolled case.

Finally, the total performance of each case in the Sylmar, Newhall, Kobe and El-Centro earthquake is calculated individually based on obtained total performance results as follows

$$P_i = \frac{1}{\text{Max}_{i=1}^4 \left( \sum_{k=1}^{19} P_i(x_k) \right)} \left( \sum_{k=1}^{19} P_i(x_k) \right) \times 100 \tag{35}$$

in which,  $P_i$  is performance of  $i^{th}$  method in reduction of the nineteen items at all stories during the four earthquakes. As demonstrated in Fig. 18.2, the proposed scheme, variable stiffness, has the maximum performance in decreasing both damages and dynamic responses of the structure in the each earthquake, significantly. The performance of passive on case is lower than the variable stiffness case and more than the other cases in the each earthquake. Also, the performance of passive off case is more than the uncontrolled case in the each earthquake except in El-Centro.

Here, the proposed control algorithm (SHM&Control) is compared with a regular semi-active control strategy (only control) for more evaluation. Thus, the semi-active control strategy based on online measurement of the interstory drift, proposed by Karami and Akbarabadi (2016), and the proposed control algorithm are evaluated and compared with the case uncontrolled structure. In the only vibration control strategy, the stiffness of the SAIVS device is obtained as follows

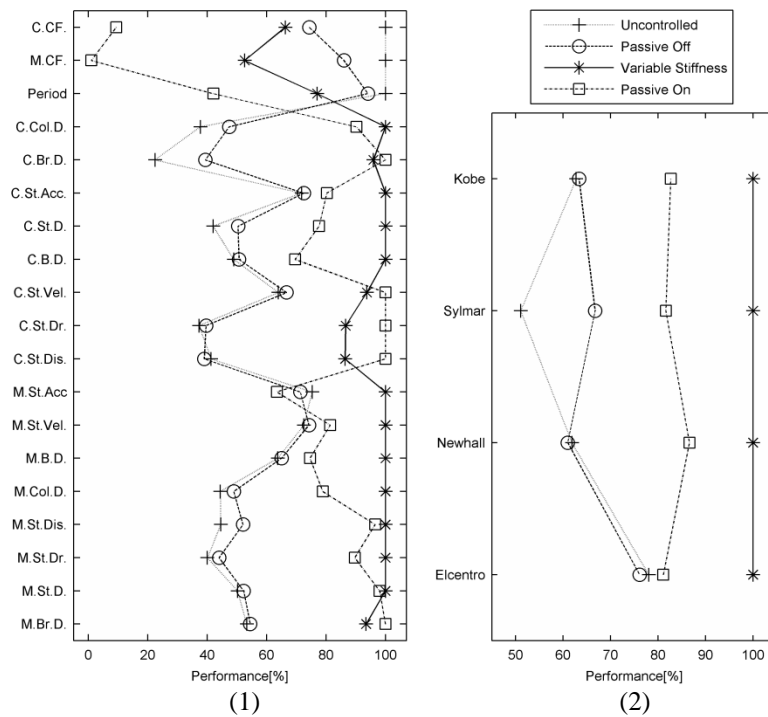


Fig. 18 Total performance of the uncontrolled, passive off, variable stiffness and passive on cases: (1) in the each 19 items based on the obtained performance results from the four earthquakes (2) in the overall 19 items during four earthquakes

$$k_{s(t)} = \begin{cases} k_{s_{\min}} & 0 \leq d_{st}(t) \leq 0.25d_{all} \\ 0.25k_{s_{\max}} & 0.25d_{all} < d_{st}(t) \leq 0.5d_{all} \\ 0.5k_{s_{\max}} & 0.5d_{all} < d_{st}(t) \leq 0.75d_{all} \\ 0.75k_{s_{\max}} & 0.75d_{all} < d_{st}(t) \leq d_{all} \\ k_{s_{\max}} & d_{all} < d_{st}(t) \end{cases} \quad (36)$$

in which,  $d_{st}(t)$  and  $d_{all}$  are the interstory drift and allowable drift, respectively, which the latter is equated to 1cm in this study. Also, a constraint is considered to prevent sudden changes in the  $k_{s(t)}$ : If (a) the necessary SAIVS device stiffness at time  $t$  is smaller than the SAIVS device stiffness at time  $t-\Delta t$ ; (b) the SAIVS device stiffness at time  $t-\Delta t$  is larger than the SAIVS device stiffness at time  $t-2\Delta t$ ; and (c) if  $d_{st}(t)\dot{d}_{st}(t) > 0$  then, the proper SAIVS device stiffness at time  $t$  is equated to the SAIVS device stiffness at time  $t-\Delta t$ .

The comparison of the displacement response time history at each story of the structure in the three cases, including the uncontrolled, the proposed semi-active control algorithm (SHM&Control) and the only vibration control strategy (control) due to the four earthquakes is demonstrated by Fig. 19. It is clear that, the proposed semi-active control could effectively decrease the maximum stories displacement in all earthquakes. The reduction of maximum stories displacement by the proposed semi-active controller is higher than the only vibration control strategy.

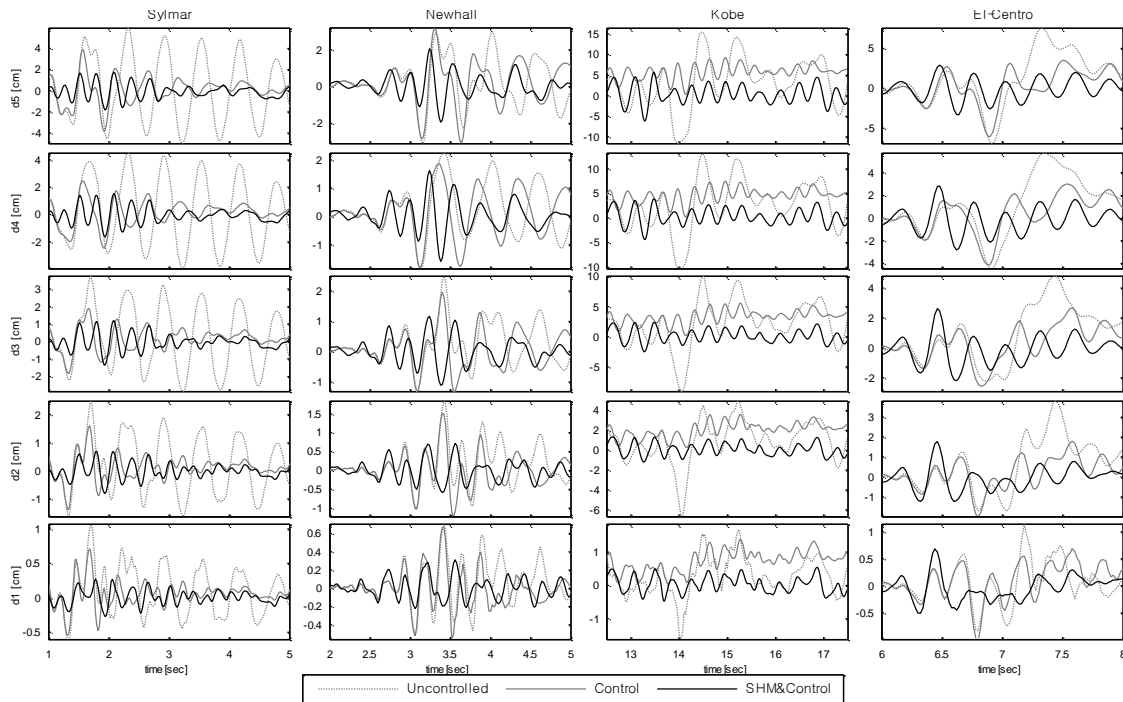


Fig. 19 The story displacement response time history under four earthquakes

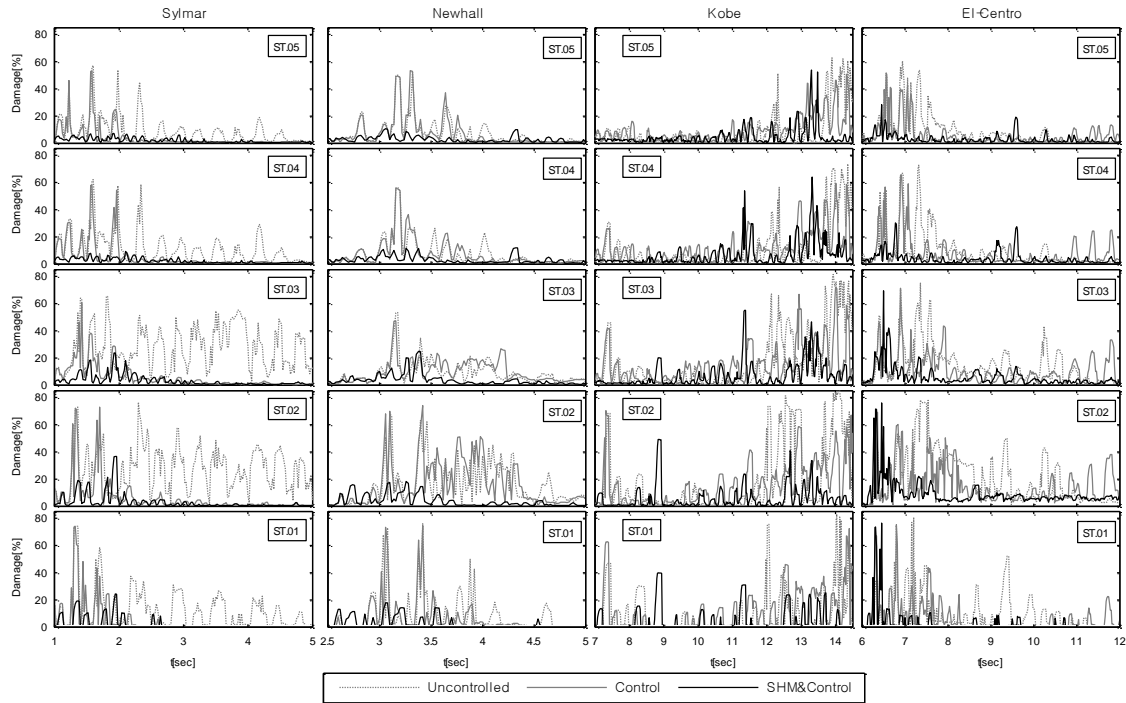


Fig. 20 Online monitoring of damage in the story lateral stiffness under four earthquakes

Also, the real-time monitoring of damage in lateral story stiffness is shown by Fig. 20. The damage in lateral story stiffness during four earthquakes is reduced remarkably by the proposed semi-active control algorithm (SHM&Control). There is permanent damage in lateral story stiffness after time 13 sec in uncontrolled structure and the only vibration control strategy (control) due to Kobe earthquake but, as shown in Fig. 20, the proposed control algorithm could reduce the damage, effectively. It is quite significant for the proposed semi-active controller in comparison with the uncontrolled case. Similar to the displacement response time history, the performance of the proposed semi-active control algorithm in decreasing the damage in lateral story stiffness is better than the only vibration control strategy.

## 7. Conclusions

In this paper application of integrated online SHM and semi-active control strategy to reduce both damage and seismic response of the main structure under strong seismic ground motion was presented. In other words, in this study the online SHM was used to enhance structural vibration control unlike the prior research studies. In this investigation, the proper stiffness selection of the SAIVS device was obtained based on damage detection in story lateral stiffness using the real time DDA/ISMP method. The obtained results showed that the proposed control algorithm could significantly decrease damage in most parts of the structure. Also, the dynamic response of the structure was effectively reduced by using the proposed control algorithm during the strong

seismic ground motion. In comparison to passive on and off cases, the results showed that the performance of the proposed control algorithm in decreasing both damage and dynamic responses of structure is significantly more. Unlike the proposed control algorithm, the passive on and off cases had the lower performance in some situations even than the uncontrolled case. Furthermore, in the energy consumption point of view the maximum and the cumulative control force in the proposed control algorithm is less than the passive on case, considerably.

In comparison to the only vibration control strategy, it was shown that the performance of the proposed control algorithm in decreasing the dynamic response of the structure and the damage in lateral story stiffness is more effective. In a regular vibration control strategy, the dynamic response of the structure is limited based on measured data. Also, there is no sense about behavior of the structure during excitation. We are facing to only measured response data and the information about probable occurred damage in the structure is not available. But, in the proposed method the SHM provides useful real time information about damage occurrence in the structure during excitation. In simple words, the remarkable difference and key point is that, identifying damage (location, type and quantity) in the proposed method plays the role of a memory which saves the recent situation of structure behavior from damage occurrence point of view during earthquake.

Finally it can be concluded that the creation of smart structure can be achieved by using the proposed algorithm. So that, the smart system identifies location and quantity of the occurred damage due to strong earthquake excitation. Then it makes proper decisions for generating control force by semi-active control devices to mitigate both damage and dynamic response of the structure.

## References

- Amini, F. and Karami, K. (2011), "Capacity design by developed pole placement structural control", *Struct. Eng. Mech.*, **39**(1), 147-168.
- Amini, F. and Karami, K. (2012), "Damage detection algorithm based on identified system Markov parameters (DDA/ISMP) in building structures with limited sensors", *Smart Mater. Struct.*, **21**(5), 055010.
- Amini, F., Mohajeri, S.A. and Javanbakht, M. (2015), "Semi-active control of isolated and damaged structures using online damage detection", *Smart Mater. Struct.*, **24**(10), 105002.
- Bitaraf, M., Barroso, L.R. and Hurlebaus, S. (2010), "Adaptive control to mitigate damage impact on structural response", *J. Intel. Mat. Syst. Str.*, **21**, 607-619.
- Cha, Y.J. and Buyukozturk, O. (2015), "Structural damage detection using modal strain energy and hybrid multiobjective optimization", *Comput. - Aided Civil Infrastruct. E.*, **30**(5), 347-358.
- Chen, B., Xu, Y. and Zhao, X. (2010), "Integrated vibration control and health monitoring of building structures: a time-domain approach", *Smart Struct. Syst.*, **6**(7), 811-833.
- Chopra, A.K. (1995), *Dynamics of Structures*, Prentice Hall, New Jersey, USA.
- Chu, S.Y. and Lo, S.C. (2009), "Application of real-time adaptive identification technique on damage detection and structural health monitoring", *Struct. Control Health Monit.*, **16**(2), 154-177.
- Gattulli, V. and Romeo, F. (2000), "Integrated procedure for identification and control of MDOF structures", *J. Eng. Mech. - ASCE*, **126**(7), 730-737.
- Huang, Q., Xu, Y.L., Li, J.C., Su, Z.Q. and Liu, H.J. (2012), "Structural damage detection of controlled building structures using frequency response functions", *J. Sound Vib.*, **331**(15), 3476-3492.
- Juang, J.N. (1994), *Applied System Identification*, Prentice Hall, Michigan, USA.
- Juang, J.N., Phan, M., Horta, L.G. and Longman, R.W. (1993), "Identification of observer/Kalman filter

- Markov parameters-Theory and experiments”, *J. Guid. Control Dynam.*, **16**(2), 320-329.
- Karami, K. and Akbarabadi, S. (2016), “Developing a smart structure using integrated subspace-based damage detection and semi-active control”, *Comput. - Aided Civil Infrastruct. E.*, **31**(11), November 2016. DOI: 10.1111/mice.12231
- Karami, K. and Amini, F. (2012), “Decreasing the damage in smart structures using integrated online DDA/ISMP and semi-active control”, *Smart Mater. Struct.*, **21**(10), 105017.
- Kim, M.H. (2002), “Simultaneous structural health monitoring and vibration control of adaptive structures using smart materials”, *Shock Vib.*, **9**(6), 329-339.
- McGuire, W., Gallagher, R.H. and Ziemian, R.D. (2000), *Matrix Structural Analysis*, Wiley.
- Nagarajaiah, S. (2000), “Structural vibration damper with continuously variable stiffness”, U.S. Patent 6098969.
- Nagarajaiah, S. and Sahasrabudhe, S. (2006), “Seismic response control of smart sliding isolated buildings using variable stiffness systems: an experimental and numerical study”, *Earthq. Eng. Struct. D.*, **35**(2), 177-198.
- Nagarajaiah, S. and Sonmez, E. (2007), “Structures with semiactive variable stiffness single/multiple tuned mass dampers”, *J. Struct. Eng. - ASCE*, **133**(1), 66-77.
- Nagarajaiah, S. and Varadarajan, N. (2005), “Short time Fourier transform algorithm for wind response control of buildings with variable stiffness TMD”, *Eng. Struct.*, **27**(3), 431-441.
- Narasimhan, S. and Nagarajaiah, S. (2005), “A STFT semiactive controller for base isolated buildings with variable stiffness isolation systems”, *Eng. Struct.*, **27**(4), 514-523.
- O’Byrne, M., Ghosh, B., Schoefs, F. and Pakrashi, V. (2014), “Regionally enhanced multiphase segmentation technique for damaged surfaces”, *Comput. - Aided Civil Infrastruct. E.* **29**(9), 644-658.
- Ray, L.R., Koh, B.H. and Tian, L. (2000), “Damage detection and vibration control in smart plates: towards multifunctional smart structures”, *J. Intel. Mat. Syst. Str.*, **11**(9), 725-739.
- Ray, L.R. and Tian, L. (1999), “Damage detection in smart structures through sensitivity-enhancing feedback control”, *Proceedings of the 1999 Symposium on Smart Structures and Materials*. International Society for Optics and Photonics.
- Sun, D. and Tong, L. (2003), “Closed-loop based detection of debonding of piezoelectric actuator patches in controlled beams”, *Int. J. Solids Struct.*, **40**(10), 2449-2471.
- Sun, H., Feng, D., Liu, Y. and Feng, M.Q. (2015), “Statistical regularization for identification of structural parameters and external loadings using state space models”, *Comput. - Aided Civil Infrastruct. E.*, **30**(11), 843-858.
- Varadarajan, N. and Nagarajaiah, S. (2004), “Wind response control of building with variable stiffness tuned mass damper using empirical mode decomposition/Hilbert transform”, *J. Eng. Mech. - ASCE*, **130**(4), 451-458.
- Viscardi, M. and Lecce, L. (2002), “An integrated system for active vibro-acoustic control and damage detection on a typical aeronautical structure”, *Control Applications, 2002. Proceedings of the 2002 International Conference on*. IEEE.
- Xu, Y. and Chen, B. (2008), “Integrated vibration control and health monitoring of building structures using semi-active friction dampers: Part I—methodology”, *Eng. Struct.*, **30**(7), 1789-1801.